

## **Supplementary Information**

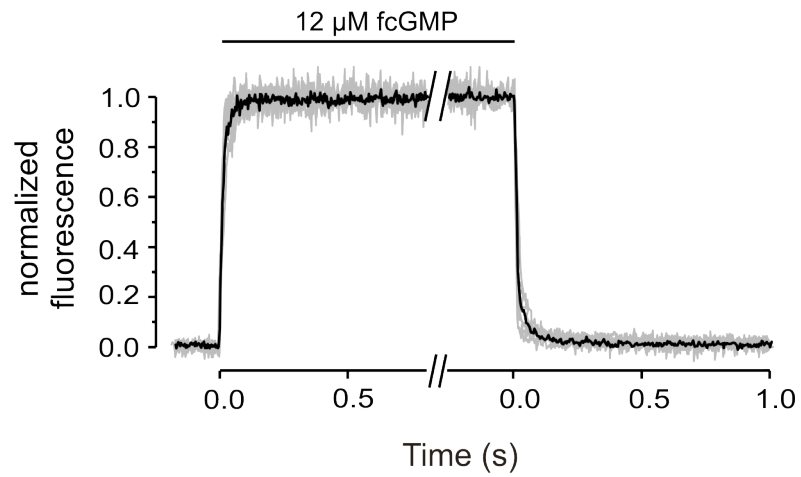
### **Hysteresis of ligand binding in CNGA2 ion channels**

by Vasilica Nache, Thomas Eick, Eckhard Schulz, Ralf Schmauder, and Klaus Benndorf\*

\* Correspondence: [Klaus.Benndorf@med.uni-jena.de](mailto:Klaus.Benndorf@med.uni-jena.de)

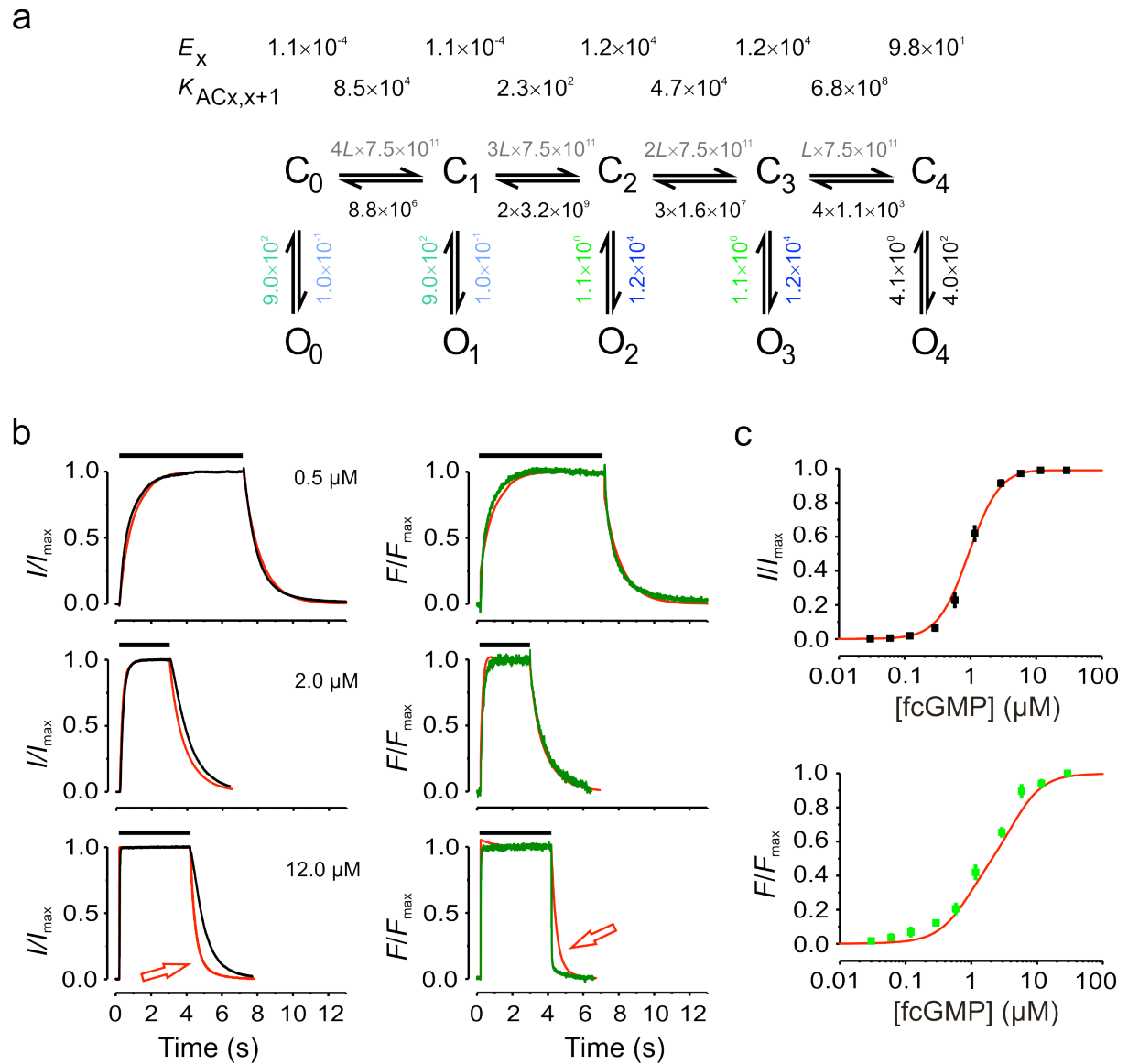
## SUPPLEMENTARY FIGURES

### Supplementary Figure S1.



**Time course of ligand binding and unbinding.** Superimposition of six normalized individual traces (grey) and the resulting respective averaged trace (black) for ligand binding and unbinding. The fcGMP concentration was stepped from 0 μM to 12 μM and back to 0 μM.

## Supplementary Figure S2.

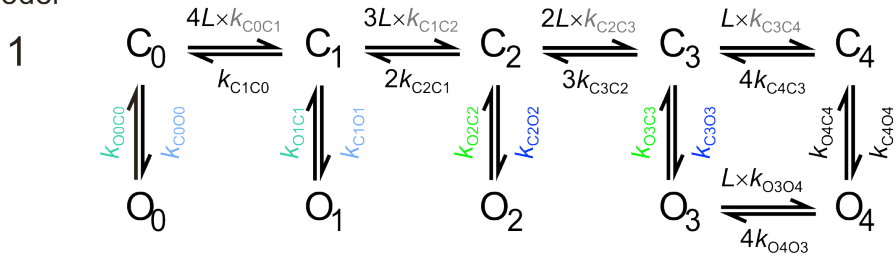


**Fit of ligand binding and unbinding as well as channel activation and deactivation with the C4L model. (a)** Scheme of the C4L model.  $C_x$  and  $O_x$  ( $x = 0 \dots 4$ ) denote closed and open states, respectively.  $L$  is a ligand. Rate constants set equal in the fit are indicated by using the same colours.  $E_x$  are the equilibrium constants for the closed-open isomerizations and  $K_{ACx,x+1}$  are equilibrium association constants. **(b)** Time courses of ligand binding and unbinding (green) as well as activation and deactivation (black) for three fcGMP concentrations. The concentration jumps from 0 to the respective fcGMP concentrations and back to 0 are

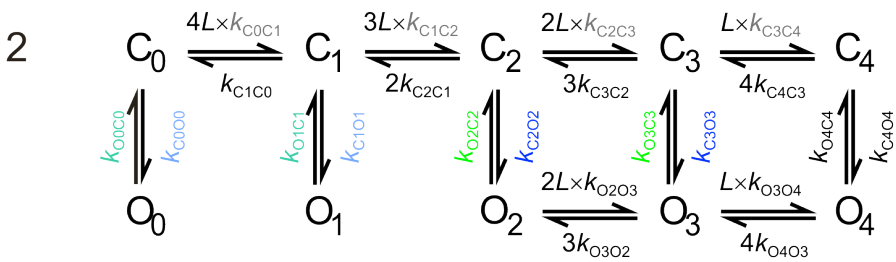
indicated by the beginning and the end of the black bar above each trace, respectively. **(c)** Steady-state relationships for activation (left, black symbols) and ligand binding (right, green symbols). The red curves in **b** and **c** are the result of the best global fit of the time courses of ligand binding, ligand unbinding, activation, and deactivation as well as the steady-state relationships with the C4L model. The model does not fit the time courses of ligand unbinding and deactivation at the same time. The reduced  $\chi_r^2$  was 21.5.

**Supplementary Figure S3.**

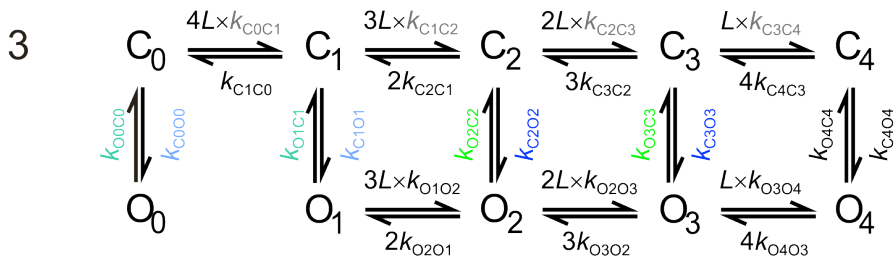
No. of model



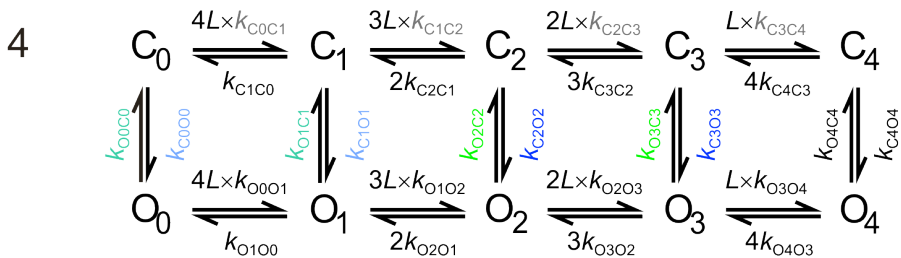
$\chi_r^2 = 27.3$   
No. of free parameters: 8



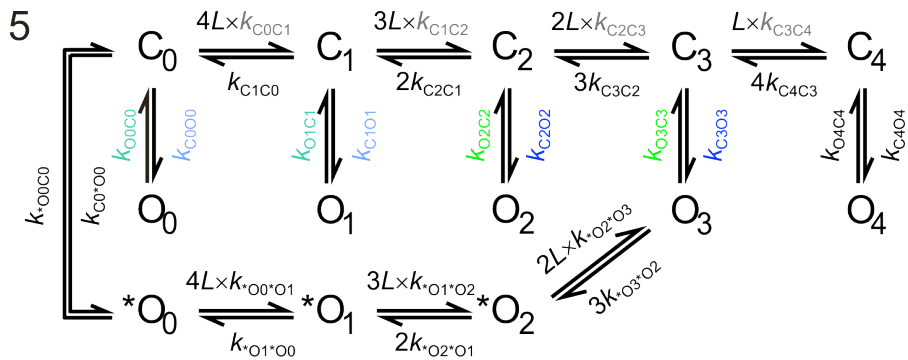
$\chi_r^2 = 14.8$   
No. of free parameters: 8



$\chi_r^2 = 21.1$   
No. of free parameters: 10

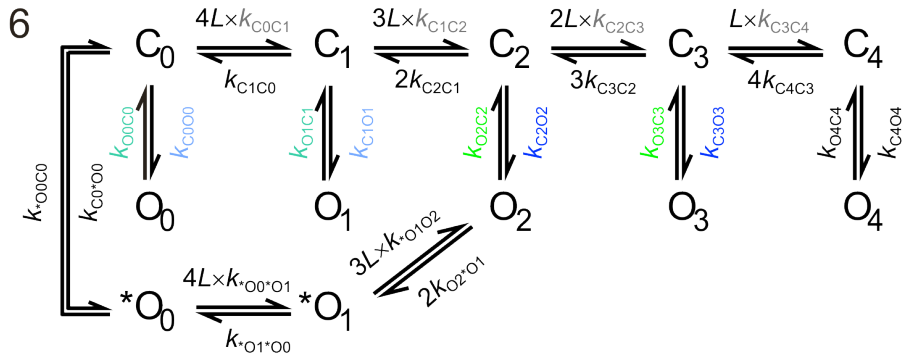


$\chi_r^2 = 15.9$   
No. of free parameters: 11

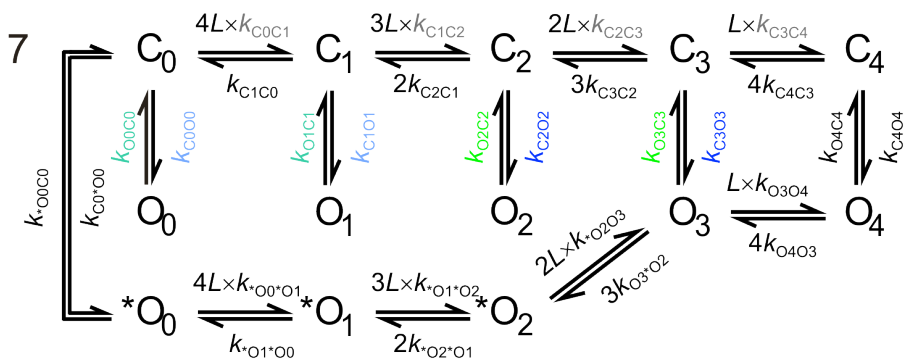


$\chi_r^2 = 14.9$   
No. of free parameters: 10

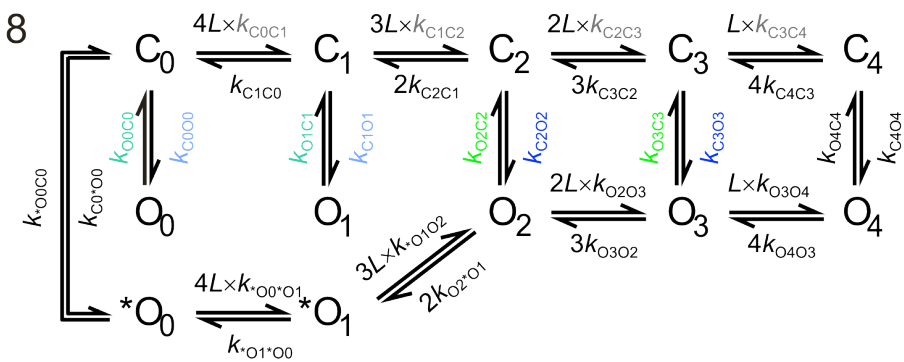
No. of model



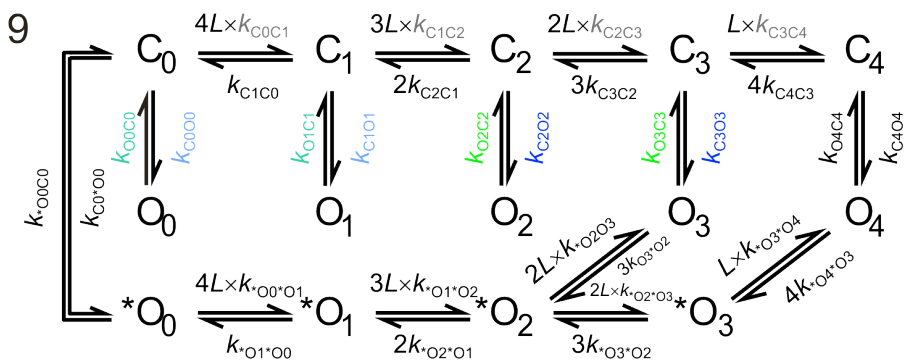
$\chi_r^2 = 20.5$   
No. of free parameters: 10



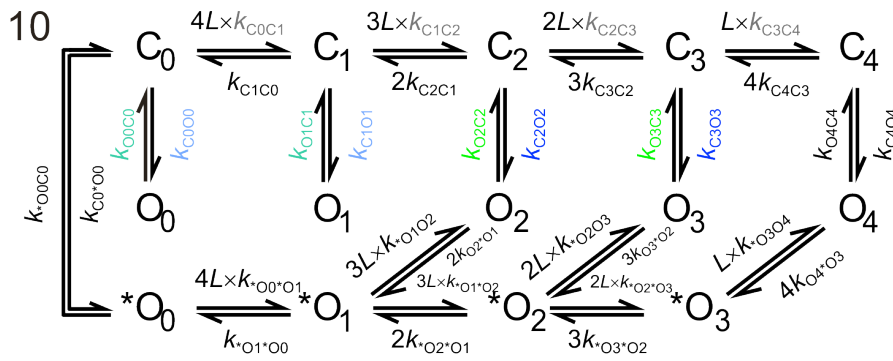
$\chi_r^2 = 6.9$   
No. of free parameters: 11



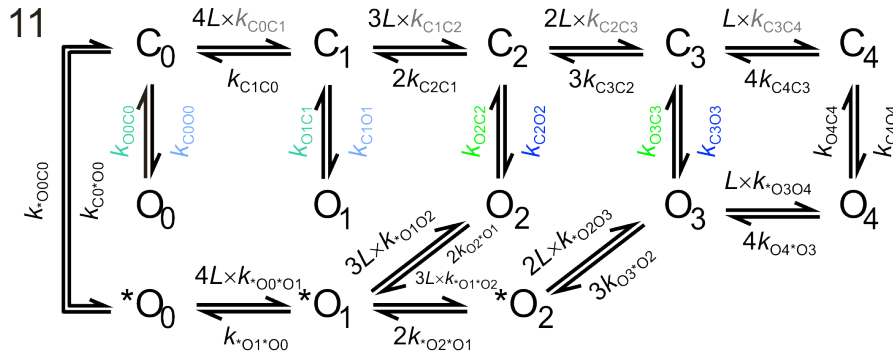
$\chi_r^2 = 12.7$   
No. of free parameters: 12



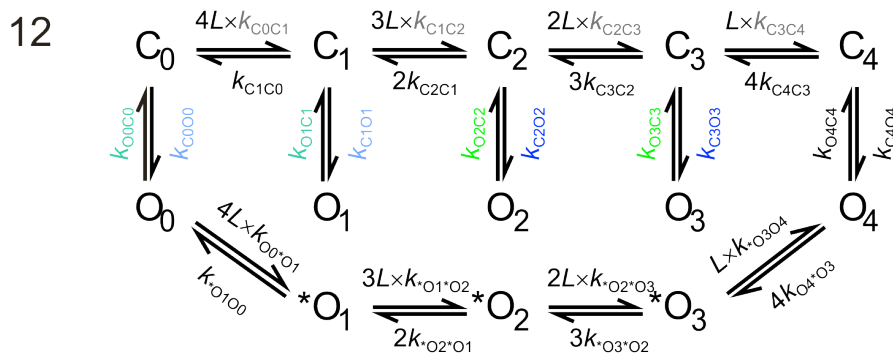
$\chi_r^2 = 7.1$   
No. of free parameters: 9



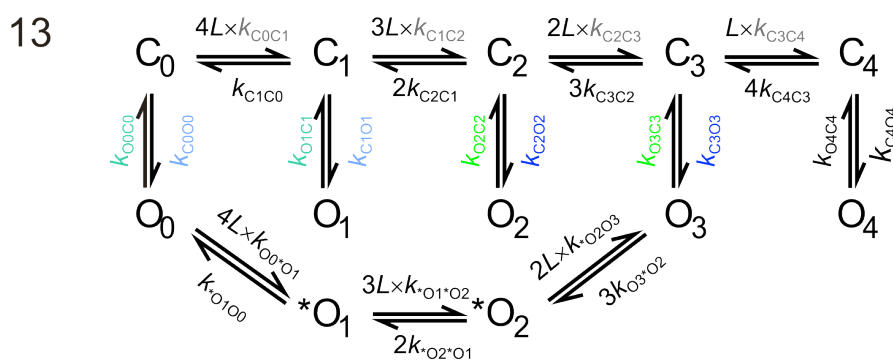
$\chi_r^2 = 40.0$   
No. of free parameters: 8



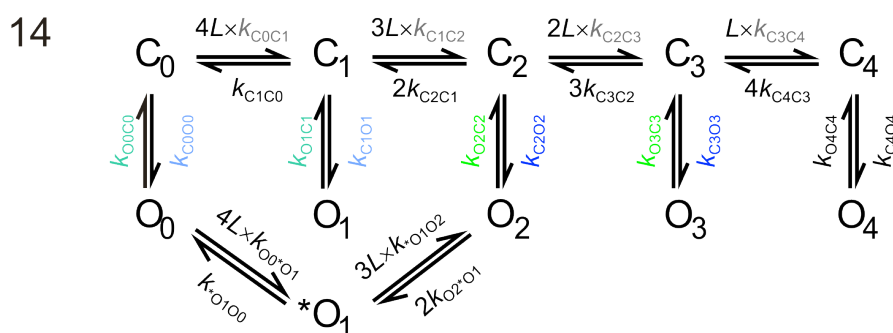
$\chi_r^2 = 27.1$   
No. of free parameters: 10



$\chi_r^2 = 12.1$   
No. of free parameters: 8



$\chi_r^2 = 19.2$   
No. of free parameters: 8



$\chi_r^2 = 18.3$   
No. of free parameters: 8

## Selection of tested alternative models with ligand unbinding via the states C<sub>x</sub>, O<sub>x</sub> and/or

\*O<sub>x</sub>. Rate constants set equal in the fitting strategy are shown in equal color. The number of parameters and the reduced  $\chi_r^2$  values of the fit are provided at the right side.

### SUPPLEMENTARY TABLES

**Supplementary Table S1.** Rate and equilibrium constants determined for the C4L model when fitting the time courses of ligand binding and channel activation in addition to the two steady-state relationships (see scheme below; Fig. 2a).

Rate constant				Equilibrium constant			
	Value	Dimension	CV (%)		Value	Dimension	CV (%)
$k_{C0C1}$	$1.5 \times 10^7$	$s^{-1}M^{-1}$	12.7	$K_{AC1}$	$1.7 \times 10^5$	$M^{-1}$	9.0
$k_{C1C0}$	$8.9 \times 10^1$	$s^{-1}$	13.9				
$k_{C1C2}$	$1.5 \times 10^7$	$s^{-1}M^{-1}$	12.7	$K_{AC2}$	$6.8 \times 10^4$	$M^{-1}$	21.5
$k_{C2C1}$	$2.2 \times 10^2$	$s^{-1}$	32.0				
$k_{C2C3}$	$1.5 \times 10^7$	$s^{-1}M^{-1}$	12.7	$K_{AC3}$	$5.6 \times 10^5$	$M^{-1}$	21.5
$k_{C3C2}$	$2.7 \times 10^1$	$s^{-1}$	25.9				
$k_{C3C4}$	$1.5 \times 10^7$	$s^{-1}M^{-1}$	12.7	$K_{AC4}$	$2.8 \times 10^5$	$M^{-1}$	20.0
$k_{C4C3}$	$5.4 \times 10^1$	$s^{-1}$	14.7				
$k_{C0O0}$	$1.0 \times 10^{-1}$	$s^{-1}$	-	$E_0$	$1.1 \times 10^{-4}$	-	-
$k_{O0C0}$	$9.0 \times 10^2$	$s^{-1}$	-				
$k_{C1O1}$	$1.0 \times 10^{-1}$	$s^{-1}$	-	$E_1$	$1.1 \times 10^{-4}$	-	-
$k_{O1C1}$	$9.0 \times 10^2$	$s^{-1}$	-				
$k_{C2O2}$	$2.4 \times 10^1$	$s^{-1}$	16.4	$E_2$	$1.9 \times 10^1$	-	16.7
$k_{O2C2}$	$1.3 \times 10^0$	$s^{-1}$	3.6				
$k_{C3O3}$	$2.4 \times 10^1$	$s^{-1}$	16.4	$E_2$	$1.9 \times 10^1$	-	16.7
$k_{O3C3}$	$1.3 \times 10^0$	$s^{-1}$	3.6				
$k_{C4O4}$	$4.0 \times 10^2$	$s^{-1}$	-	$E_4$	$9.9 \times 10^1$	-	-
$k_{O4C4}$	$4.1 \times 10^0$	$s^{-1}$	-				

The values of the rate constants were determined by the global fit as described in Supplementary Methods. The denomination corresponds to that in Fig. 2.  $k_{O0C0} = 9.0 \times 10^2 s^{-1}$ ,  $k_{C0O0} = 1.0 \times 10^{-1} s^{-1}$ ,  $k_{O4C4} = 4.1 \times 10^0 s^{-1}$ ,  $k_{C4O4} = 4.0 \times 10^2 s^{-1}$  were taken from single-channel experiments<sup>10</sup>. The equilibrium association constants,  $K_{ACx}$ , were obtained by dividing a binding rate constant by the corresponding unbinding rate constant. The equilibrium constants for the closed-open isomerizations,  $E$ , were obtained by dividing an opening rate constant by



the corresponding closing rate constant. The coefficient of variation of each parameter,  $CV$ , indicates the standard error in %. These values were taken from the main diagonal of the covariance matrix of the fit. In the fit the following rate constants were set equal:  $k_{C0C1} = k_{C1C2} = k_{C2C3} = k_{C3C4}$ ,  $k_{C1O1} = k_{C0O0}$ ,  $k_{O1C1} = k_{O0C0}$ ,  $k_{C2O2} = k_{C3O3}$ ,  $k_{O2C2} = k_{O3C3}$ .

**Supplementary Table S2.** Rate and equilibrium constants determined for the C4L-\*O4L model (see scheme below; Fig. 3a).

Rate constant				Equilibrium constant			
	Value	Dimension	$CV$ (%)		Value	Dimension	$CV$ (%)
$k_{C0C1}$	$1.8 \times 10^7$	$s^{-1}M^{-1}$	18.1	$K_{AC1}$	$1.6 \times 10^5$	$M^{-1}$	9.3
$k_{C1C0}$	$1.1 \times 10^2$	$s^{-1}$	17.9				
$k_{C1C2}$	$1.8 \times 10^7$	$s^{-1}M^{-1}$	18.1	$K_{AC2}$	$8.2 \times 10^4$	$M^{-1}$	25.8
$k_{C2C1}$	$2.2 \times 10^2$	$s^{-1}$	41.1				
$k_{C2C3}$	$1.8 \times 10^7$	$s^{-1}M^{-1}$	18.1	$K_{AC3}$	$2.4 \times 10^5$	$M^{-1}$	19.8
$k_{C3C2}$	$7.4 \times 10^1$	$s^{-1}$	30.7				
$k_{C3C4}$	$1.8 \times 10^7$	$s^{-1}M^{-1}$	18.1	$K_{AC4}$	$5.1 \times 10^5$	$M^{-1}$	23.4
$k_{C4C3}$	$3.5 \times 10^1$	$s^{-1}$	11.7				
$k_{C0O0}$	$1.0 \times 10^{-1}$	$s^{-1}$	-	$E_0$	$1.1 \times 10^{-4}$	-	-
$k_{O0C0}$	$9.0 \times 10^2$	$s^{-1}$	-				
$k_{C1O1}$	$1.0 \times 10^{-1}$	$s^{-1}$	-	$E_1$	$1.1 \times 10^{-4}$	-	-
$k_{O1C1}$	$9.0 \times 10^2$	$s^{-1}$	-				
$k_{C2O2}$	$2.3 \times 10^1$	$s^{-1}$	19.9	$E_2$	$2.1 \times 10^1$	-	21.0
$k_{O2C2}$	$1.1 \times 10^0$	$s^{-1}$	2.2				
$k_{C3O3}$	$2.3 \times 10^1$	$s^{-1}$	19.9	$E_3$	$2.1 \times 10^1$	-	21.0
$k_{O3C3}$	$1.1 \times 10^0$	$s^{-1}$	2.2				
$k_{C4*O4}$	$4.0 \times 10^2$	$s^{-1}$	-	$E_4$	$9.9 \times 10^1$	-	-
$k_{*O4C4}$	$4.1 \times 10^0$	$s^{-1}$	-				
$k_{*O3*O4}$	$6.0 \times 10^8$ #	$s^{-1}M^{-1}$	-	n.d.			
$k_{*O4*O3}$	$2.5 \times 10^1$	$s^{-1}$	24.9				
$k_{*O2*O3}$	$6.0 \times 10^8$ #	$s^{-1}M^{-1}$	-	n.d.			
$k_{*O3*O2}$	$2.5 \times 10^1$	$s^{-1}$	24.9				
$k_{*O1*O2}$	$6.0 \times 10^8$ #	$s^{-1}M^{-1}$	-	n.d.			
$k_{*O2*O1}$	$2.5 \times 10^1$	$s^{-1}$	24.9				
$k_{*O0*O1}$	$6.0 \times 10^8$ #	$s^{-1}M^{-1}$	-	n.d.			
$k_{*O1*O0}$	$2.5 \times 10^1$	$s^{-1}$	24.9				
$k_{C0*O0}$	$6.4 \times 10^{-7}$	$s^{-1}$	97.6	n.d.			
$k_{*O0C0}$	$1.2 \times 10^0$	$s^{-1}$	3.8				

# indicates that the values were set to the diffusion limit<sup>18</sup> (see text); n.d. means not determined.

The nomenclature corresponds to that in Supplementary Table S1.

## SUPPLEMENTARY METHODS

**Fitting kinetic models.** To determine the rate and/or equilibrium constants for a given model, the averaged and normalized time courses of binding/unbinding and of activation/deactivation, each at 0.5, 2.0, and 12.0  $\mu\text{M}$  fcGMP, were globally fitted (Figs. 2,3; Supplementary Figs. S2, S3) by using a modified Levenberg-Marquardt algorithm<sup>45</sup>. The goodness of the fit was determined by the  $\chi^2$  value computed for the normalized current amplitudes,  $I_m(t_j, x_i)$ , and fluorescence intensities,  $F_m(t_j, x_i)$ , and the respective theoretical values,  $I_c(t_j, x_i)$  and  $F_c(t_j, x_i)$ , at time  $t_j$  and concentration  $x_i$ .

$$\chi^2 = g \left[ \sum_{i=1}^{n_t} \sum_{j=1}^{n_d} \frac{(F_m(t_j, x_i) - F_c(t_j, x_i))^2}{\sigma_F^2(t_j, x_i)} + \sum_{i=1}^{n_t} \sum_{j=1}^{n_d} \frac{(I_m(t_j, x_i) - I_c(t_j, x_i))^2}{\sigma_I^2(t_j, x_i)} \right] \quad (\text{S1})$$

$$+ \sum_{i=1}^{n_s} \frac{(Po_m(x_i) - Po_c(x_i))^2}{\sigma_{Po}^2(x_i)} + \sum_{i=1}^{n_s} \frac{(Bi_m(x_i) - Bi_c(x_i))^2}{\sigma_{Bi}^2(x_i)}$$

The trace number,  $n_t$ , denotes the number of concentrations analyzed. Its value was 3. The square of the deviations at  $t_j$  and  $x_i$  is weighted by the reciprocal values of the observed variance  $\sigma_F^2(t_j, x_i)$  and  $\sigma_I^2(t_j, x_i)$ , respectively.  $Po_m(x_i)$  and  $Bi_m(x_i)$  are the steady-state values of the open probability and normalized fluorescence intensity (degree of binding), respectively, at the concentration  $x_i$  ( $n_s = 10$ ).  $Po_c(x_i)$  and  $Bi_c(x_i)$  are the respective calculated data points. Also the squared deviations of these steady-state values were weighted by the variance  $\sigma_{Po}^2(x_i)$  and  $\sigma_{Bi}^2(x_i)$ , respectively. Because in the time courses the number of points to be fitted is much bigger than those in the steady-state relationships, we employed the factor  $g = n_s/(n_d \times n_t)$  to give the time courses and the steady-state relationships the same weight in the fit.

For the fit the equation

$$\frac{d\mathbf{p}(t)}{dt} = \mathbf{p}(t) \cdot \mathbf{Q}(x) \quad (\text{S2})$$

was solved.  $\mathbf{p}(t)$  is the row-vector of the probabilities to be in one of the states  $O_0$  to  $O_3$ ,  $*O_0$  to  $*O_4$ ,  $C_0$  to  $C_4$ , here arranged for the C4L-\*O4L model, and  $\mathbf{Q}(x)$  is the  $\mathbf{Q}$ -matrix depending on the concentration  $x$ . The computations were performed with the Eigenvalue method. The sum of the probabilities of all open states is the open probability  $Po(t)$ , which was calculated by multiplication with the column vector  $\mathbf{u}_o$ , consisting of ones and zeros for the opened and closed states, respectively  $\mathbf{u}_o = (1,1,1,1,1,1,1,1,1,0,0,0,0,0)^T$ . The normalized current values were assumed to correspond to the calculated  $Po(t)$  according to  $I_c(t) = \mathbf{p}(t) \cdot \mathbf{u}_o$ . The theoretical total amount of binding as function of time according to our model was obtained by including the states weighted with the factors 0, 0.25, 0.5, 0.75 and 1, depending on the number of ligands bound. The total amount of binding, computed by summing up these weighted values, was assumed to be proportional to the observed fluorescence. The most convenient way of calculating the amount of binding was to use a vector  $\mathbf{u}_B$ , which depends on the actual model, e.g.  $\mathbf{u}_B = \frac{1}{4}(0,1,2,3,0,1,2,3,4,0,1,2,3,4)^T$  for the C4L-\*OL model. The total amount of binding was calculated by  $F_c(t) = \mathbf{p}(t) \cdot \mathbf{u}_B$ .

For the time courses of ligand binding and unbinding, the rates for the confocal images were 182 Hz at 0.5  $\mu\text{M}$  cGMP, 277 Hz at 2.0  $\mu\text{M}$  cGMP, and 277 Hz at 12.0  $\mu\text{M}$  cGMP. Because one confocal image provided one sampling point in the traces of ligand binding and unbinding, this resulted in sampling intervals of 5.5 ms, 3.6 ms, and 3.6 ms respectively. For the fit of the respective time courses of activation and deactivation, data points were computed by an interpolation routine which exactly matched the time of the data points in the traces of binding and unbinding. Finally 33 data points were selected for each time course of binding, unbinding, activation, and deactivation to fully describe the phase of amplitude

change in all time courses. Hence, each trace had  $n_d = 66$  points to be fitted, resulting in  $2 \times n_d \times n_t = 2 \times 66 \times 3 = 396$  data points arising from the time courses to be used in the global fit.

In our fit procedure, the time courses of ligand binding and activation were not fitted with their absolute amplitude. Instead they were normalized with respect to the late amplitude in the presence of the ligand. The same normalization was used for the corresponding time courses of unbinding and deactivation. Hence, in the fit the “shape” of the traces was fitted.

In addition to the traces, ligand binding and activation under steady-state conditions was included by 10 data points each, covering the concentration range between 0.03 and 29.1  $\mu\text{M}$  fcGMP (Figs. 2c, 3c, and Supplementary Fig. S2). In the global fit the total of the traces and the total of steady steady-state values were weighted by 50% each, thereby weighting each of the 396 sampling points with  $g = n_s / (n_d \times n_t) = 0.05$ . This means, that the effective number of points to be fitted in the current- and fluorescence time courses equals the number of the concentrations values in the steady-state data,  $n_s$ . The fitting procedure minimized  $\chi^2$ .

The reduced  $\chi^2$  value for the global fit was obtained by dividing  $\chi^2$  by the degrees of freedom of the fit according to

$$\chi_r^2 = \frac{\chi^2}{4n_s - m} \quad (\text{S3})$$

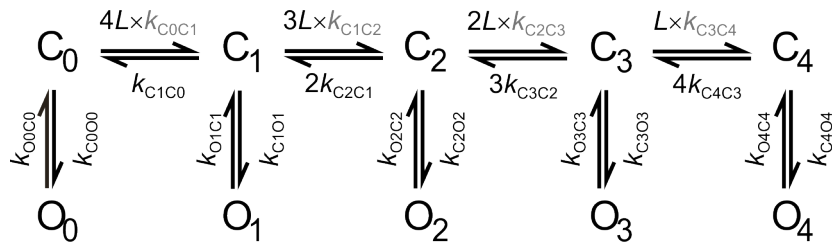
$n_s$  is the number of sampling points in the steady-state binding and steady-state activation as well as the effective number of points of the theoretical current- and fluorescence time courses.  $m$  is the number of parameters. If only random errors contribute to the scattering of the data and if the model fits to the data, then the reduced  $\chi^2$  value should approximate unity. With the unusual stringency in our global fits, the best value for the C4L-\*O4L model was about 6.0 (Fig. 3). The standard errors of the fitted parameters were obtained from the covariance matrix and the  $\chi^2$  hypersurface.

Some further general rules were adopted for the fit:

1. In models containing cycles, the principle of microscopic reversibility was taken into account. This means that within a cycle the product of the rate constants in the forward direction equals the product of the rate constants in the backward direction. This reduced the number of rate constants to be fitted in each cycle by one.
2. If rate constants were not determined with reasonable accuracy (standard error > 45%), equally directed rate constants were equated and it was then tested whether the quality of the fit (evaluated by  $\chi^2$ ) was kept. If  $\chi^2$  was not increased by equating two rate constants, the manoeuvre was accepted.
3. The transitions  $C_2 \leftrightarrow O_2$  and  $C_3 \leftrightarrow O_3$  were assumed to be equal because the fit did not allow us to differentiate them.

**Calculation of the rate constants with the C4L model.** The C4L model described previously<sup>10</sup> for the steady-state binding and activation by fcGMP as well as activation gating by cGMP is shown in the following scheme.

Scheme of the C4L model



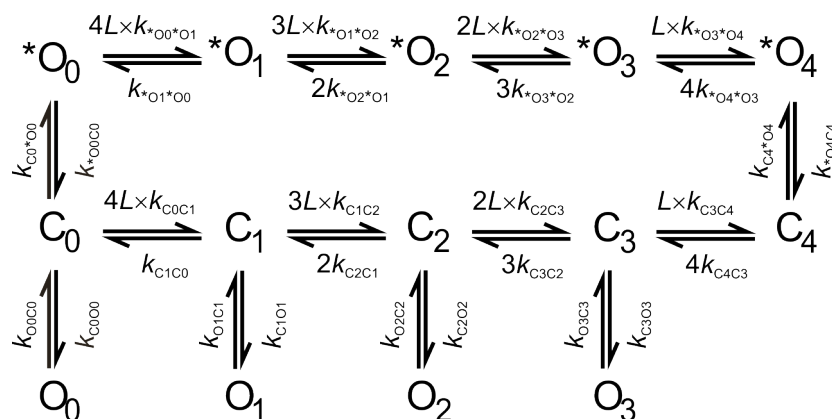
Closed and open states are symbolized by  $C_x$  and  $O_x$ , respectively.  $L$  is the ligand concentration in M. The rate constants,  $k_{XY}$ , characterize the transitions from state X to state Y. Their values at zero and saturating fcGMP were taken from single-channel experiments<sup>10</sup> to be  $k_{O_0C_0} = 9.0 \times 10^2 \text{ s}^{-1}$ ,  $k_{C_0O_0} = 1.0 \times 10^{-1} \text{ s}^{-1}$ ,  $k_{O_4C_4} = 4.1 \times 10^0 \text{ s}^{-1}$ ,  $k_{C_4O_4} = 4.0 \times 10^2 \text{ s}^{-1}$ , resulting in closed-open isomerization constants  $E_0 = k_{C_0O_0}/k_{O_0C_0} = 1.1 \times 10^{-4}$  and  $E_4 = k_{C_4O_4}/k_{O_4C_4} = 9.9 \times 10^1$ , respectively. When setting the remaining 14 rate constants as free

parameters, their determinateness was only poor. Similar to our previous report<sup>10</sup> we next reduced the number of free parameters to 8 by setting the following parameters equal:  $k_{C0C1} = k_{C1C2} = k_{C2C3} = k_{C3C4}$ . Assumed was further  $k_{C2O2} = k_{C3O3}$  and  $k_{O2C2} = k_{O3C3}$ , resulting in  $E_2 = E_3$ . The resulting fit led to a reasonable determinateness of all parameters apart from  $k_{C1O1}$  and  $k_{O1C1}$ . Because it turned out in all fits that  $k_{C1O1} \gg k_{O1C1}$  we further simplified the fit by setting  $k_{C1O1} = k_{C0O0}$  and  $k_{O1C1} = k_{O0C0}$ , i.e.  $E_1 = E_0$ . This resulted in a fit with only 7 free parameters that were fully determined (Fig. 2a; Supplementary Table S1). Notably, the goodness of the fit did not significantly worsen by reducing the parameter number from 14 to 7, suggesting that the shown deficiencies preferably in the unbinding and deactivation did not depend on a limited number of free parameters but on the structure of the model. The approach described for the C4L model holds in an analogue fashion also for the other tested models.

In all further models tested, we set  $k_{O0C0} = 9.0 \times 10^2 \text{ s}^{-1}$ ,  $k_{C0O0} = 1.0 \times 10^{-1} \text{ s}^{-1}$ ,  $k_{O4C4} = 4.1 \times 10^0 \text{ s}^{-1}$ ,  $k_{C4O4} = 4.0 \times 10^2 \text{ s}^{-1}$ ,  $k_{C0C1} = k_{C1C2} = k_{C2C3} = k_{C3C4}$ ,  $k_{C1O1} = k_{C0O0}$ ,  $k_{O1C1} = k_{O0C0}$ ,  $k_{C2O2} = k_{C3O3}$  and  $k_{O2C2} = k_{O3C3}$ .

**Calculation of the rate constants with the C4L-\*O4L model.** The following scheme shows the C4L-\*O4L model, which described our data best.

Scheme of the C4L-\*O4L model



The states  $*O_x$  describe a pathway which is practically solely used for deactivation. The rate constants at zero and saturating fcGMP were set as described for the C4L model. This was justified because the  $*O$ -pathway is quantitatively only recruited during deactivation after removing the ligand but not during activation, i.e. in the presence of the ligand (see Fig. 6).

**Computation of net probability flux densities.** The net probability flux density for the four binding steps in the C4L- $*O4L$  model of the channel in the closed and open conformation were computed by

$$f_{C_{x-1}C_x}(t) = L \times k_{C_{x-1}C_x} \times C_{x-1}(t) - k_{C_x C_{x-1}} \times C_x(t) \quad (x = 1 \dots 4) \quad (S4)$$

and 
$$f_{*O_{x-1}*O_x}(t) = L \times k_{*O_{x-1}*O_x} \times *O_{x-1}(t) - k_{*O_x *O_{x-1}} \times *O_x(t) \quad (x = 1 \dots 4) \quad (S5)$$

respectively. For the closed-open isomerizations the net probability flux density was obtained by

$$f_{C_x O_x}(t) = k_{C_x O_x} \times C_x(t) - k_{O_x C_x} \times O_x(t) \quad (x = 0 \dots 3) \quad (S6)$$

$$f_{C_0 *O_0}(t) = k_{C_0 *O_0} \times C_0(t) - k_{*O_0 C_0} \times *O_0(t) \quad (S7)$$

and 
$$f_{C_4 *O_4}(t) = k_{C_4 *O_4} \times C_4(t) - k_{*O_4 C_4} \times *O_4(t), \quad (S8)$$

respectively. The procedure has been described in detail previously<sup>13</sup>.

The total net probability fluxes between two neighbored states,  $F_{XY}$ , were obtained by computing the following time integral

$$F_{XY} = \int_{t=0}^{t_{\text{end}}} f_{XY} dt \quad (S9)$$

For ligand binding and activation  $t_0$  is the time at which the ligand was applied and  $t_{\text{end}}$  the time just before the ligand was removed. Correspondingly, for ligand unbinding and deactivation  $t_0$  is the time at which the ligand was removed and  $t_{\text{end}}$  the time at the end of the recording. Hence,  $F_{XY}$  indicates how much of the total net probability flux moves along a transition  $X \leftrightarrow Y$ .

**Transition pathway analysis.** If a Markovian model is fully reversible, the total probability flux can easily be decomposed into the pathway net probability fluxes as described previously for HCN2 channels<sup>13</sup>. In brief, to analyze the pathway  $p$  from state  $X_0$  to state  $X_k$  along the states  $X_i$ , first the net probability flux  $F_{p,X_0X_k}$  is computed according to

$$F_{p,X_0X_k} = \min | [F_{X_{i-1}X_i} | i = 1 \dots k] | \quad (\text{S10})$$

Then  $F_{p,X_0X_k}$  is subtracted from the flux along all edges of this pathway  $p$ . Then the analysis procedure is repeated for the remaining pathways until the total probability flux between these states is zero<sup>46</sup>. A useful approach is to start with the strongest pathway<sup>46</sup>.

Consider, for example, at 12  $\mu\text{M}$  fcGMP the transition pathways  $C_0 \rightarrow *O_4$ ,  $C_0 \rightarrow O_3$ ,  $C_0 \rightarrow O_2$

(red arrows in Fig. 6A). The net probability fluxes of interest are  $F_{C_0C_1} = 0.9995$ ,

$F_{C_1C_2} = 0.9980$ ,  $F_{C_2C_3} = 0.9397$ ,  $F_{C_3C_4} = 0.8269$ ,  $F_{C_2O_2} = 0.0555$ ,  $F_{C_3O_3} = 0.1076$ ,

$F_{C_4*O_4} = 0.8188$ . First, the flux along the pathway  $C_0 \rightarrow *O_4$  was computed by

$F_{p,C_0*O_4} = \min | [F_{C_0C_1}, F_{C_1C_2}, F_{C_2C_3}, F_{C_3C_4}, F_{C_4*O_4}] | = 0.82$ . This value was then subtracted

from  $F_{C_0C_1}$ ,  $F_{C_1C_2}$ , and  $F_{C_2C_3}$ , yielding  $F_{C_0C_1}'$ ,  $F_{C_1C_2}'$ , and  $F_{C_2C_3}'$ , respectively. Then the flux along the pathway  $C_0 \rightarrow O_3$  was obtained by

$F_{p,C_0O_3} = \min | [F_{C_0C_1}', F_{C_1C_2}', F_{C_2C_3}', F_{C_3O_3}] | = 0.11$ . The flux along the pathway  $C_0 \rightarrow O_2$  was

obtained in an analogue fashion. The result does not depend on the sequence starting with the strongest pathway.

## SUPPLEMENTARY REFERENCES

45. Brown, K.M. & Dennis, J.E. Derivative-free analogues of the Levenberg-Marquardt and Gauss algorithmus or nonlinear least squares approximation. Num. Math. 18, 289-297 (1972).
46. Prinz, J.H., Keller, B. & Noe, F. Probing molecular kinetics with Markov models: metastable states, transition pathways and spectroscopic observables. Physical chemistry chemical physics : PCCP 13, 16912-27 (2011).